JOURNAL OF MATERIALS SCIENCE 26 (1991) 2071–2075

# Phase decomposition of liquid-quenched β-type Ti–Cr alloys

YOICHI IKEMATSU*, MINORU DOI, TORU MIYAZAKI
*Department of Materials Science and Engineering, Metals Section, Nagoya Institute of Technology, Gokiso-Cho, Showa-Ku, Nagoya 466, Japan*

Phase decomposition behaviour of liquid-quenched β (bcc) type Ti–Cr alloys was investigated by means of transmission electron microscopy and hardness measurements. It was found that decomposition of β to $\beta_1$ (Ti-rich, bcc) + $\beta_2$ (Ti-lean, bcc) takes place in the intermediate composition range of the Ti–Cr system. This experimental result proves the theoretical prediction made by Menon and Aaronson, but the observed $\beta_1 + \beta_2$ two-phase field expands towards higher temperatures than the predicted binodal line. The coherent $\beta_1 + \beta_2$ two-phase state exhibits the so-called ⟨1 0 0⟩ modulated structure and it was concluded that the formation of such a structure is a result of spinodal decomposition of the β-phase. We obtained time–temperature–transformation (TTT) diagrams of β-type Ti–30, 40 and 50 at % Cr alloys. A typical sequence of structural change is β → coherent $\beta_1 + \beta_2$ → incoherent $\beta_1 + \beta_2$ → incoherent $\beta_1 + \beta_2$ + grain boundary precipitates → stable state of β + $TiCr_2$ or α + $TiCr_2$. Not all the states in the above sequence appear, depending on alloy composition, liquid-quenching rate and ageing temperature.

## 1. Introduction

Ti alloys are divided into the three groups: α-type (hcp), β-type (bcc) and α–β two-phase type. Most of the Ti alloys which are now being used in practice, are α or α–β-type, but β-type is now attracting a great deal of attention because it is becoming clearer that β-phase has potentially both high strength and the good quality of being cold-workable.

It used to be believed that β-phase in Ti alloys hardly decomposed to two β-phases, i.e. Ti-rich $\beta_1$ and Ti-lean $\beta_2$ phases which have bcc structure. In fact, no two-phase field of $\beta_1 + \beta_2$ can be seen in the phase diagrams of binary Ti alloys such as Ti–Mo, Ti–V, etc, which Hansen and Anderko [1] summarized. Since then, a number of investigators, e.g. Harmon and Troiano [2], Miyagi and Shin [3], and Terauchi *et al.* [4], have shown through either experiments or theoretical calculations that the decomposition of β-phase does take place in Ti–Mo and Ti–V alloys. Hence the phase diagrams of those alloy systems, which were newly summarized by Massalski *et al.* [5], and Murray [6], have the monotectoid reaction from β to $\beta_1 + \beta_2$.

In Ti–Cr binary alloys, Narayanan *et al.* [7], Chandrasakaran *et al.* [8], and Miyagi and Shin [3] have shown the decomposition of metastable β to $\beta_1 + \beta_2$. Cr-contents of the alloys which have been studied so far, were relatively low (at most 20 at %). Menon and Aaronson [9] theoretically calculated the binodal and the spinodal lines for β-type Ti–Cr alloys. They suggested the possibility that spinodal decomposition takes place in the intermediate composition range of the Ti–Cr system. The decomposition behaviour in such an intermediate range, however, has not yet been cleared experimentally.

The aims of the present study were:

1. to investigate the phase decomposition behaviour of β-type Ti–Cr alloys by means of transmission electron microscopy (TEM) and micro-Vickers hardness measurements,
2. to draw the time–temperature–transformation (TTT) diagrams for the β-type Ti–Cr alloys based on TEM observations, and
3. to discuss the possibility of spinodal decomposition of the β-phase.

## 2. Experimental procedure

Four kinds of Ti–Cr alloys containing 30, 40, 50 and 60 at % Cr were used in the present studies. A button-like specimen (about 15 g weight) of each alloy was prepared by arc melting in an argon atmosphere. Rod specimens, each weighing about 2 g, were cut from the individual buttons. The rod specimen was melted at high temperature, and the melt was rapidly quenched (liquid-quenched) using a single-roll method to obtain the β one-phase state. For the Ti–30Cr and Ti–40Cr alloys (at %), sheet samples were cut from the individual buttons.

Liquid-quenched ribbon samples were sealed in, using a fused silica tube evacuated to the order of $10^{-5}$ Pa, and were aged at various temperatures be-

*Present address*: R and D Laboratories-I, Nippon Steel Corporation, Kawasaki 211, Japan.

0022–2461/91 $03.00 + .12 

tween 673 and 1173 K. Sheet samples, which were sealed in by the same procedure, were solution-treated in the β one-phase field, quenched into iced brine and aged. Changes in structure and hardness during ageing were examined by means of TEM observations and micro-Vickers hardness measurements.

## 3. Changes in structure and micro-Vickers hardness

### 3.1. Hardness changes

Fig. 1 illustrates the changes in micro-Vickers hardness during ageing of Ti–30Cr and Ti–40Cr alloys. Age-hardening can be seen for both liquid-quenched ribbons and the sheets quenched from the β one-phase field. In particular, ribbon samples exhibit a remarkable increase in hardness at an early stage of ageing. Hence it is highly probable that a certain kind of phase decomposition actually takes place in Ti–Cr alloys.

### 3.2. Structural changes observed with TEM

Fig. 2 shows transmission electron micrographs and the 200 reflection spots in the selected area diffraction (SAD) patterns of as-liquid-quenched Ti–Cr ribbons. For 30, 40 and 50 at % Cr ribbons, very fine contrast exists in the micrographs, and the 200 reflection spot is accompanied by satellites along ⟨100⟩ in the SAD patterns. These facts clearly indicate that $\beta \rightarrow \beta_1 + \beta_2$ decomposition takes place and $\beta_1$ and $\beta_2$ coexist coherently. For the 60 at % Cr ribbon, however, the stable phase of $TiCr_2$ has already appeared even in the as-liquid-quenched state, and the $\beta_1 + \beta_2$ two-phase state cannot be observed at all.

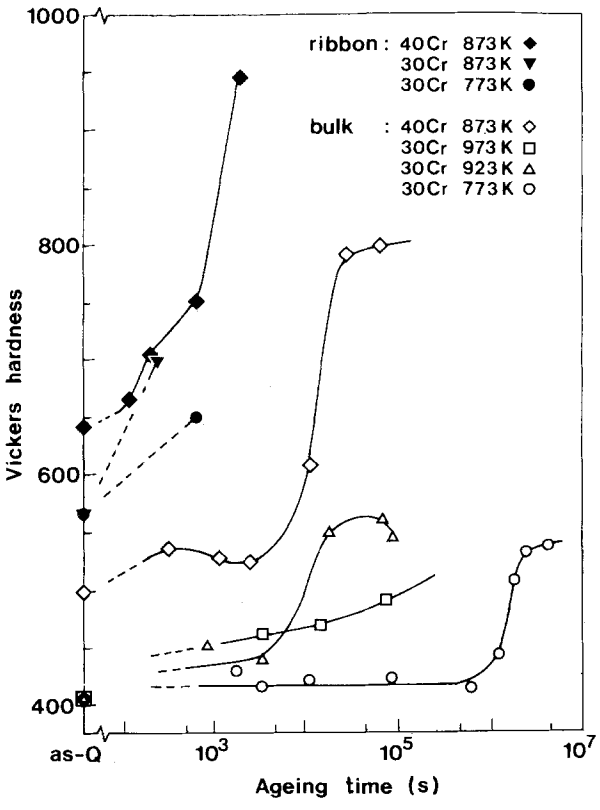


*Figure 1* Age-hardening curves of Ti–30 at % Cr and Ti–40 at % Cr alloys.

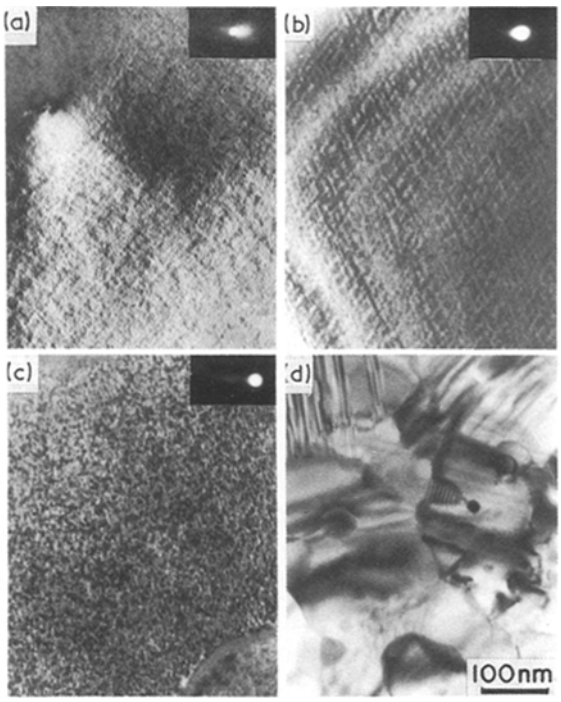


*Figure 2* TEM images and SAD patterns of as-liquid-quenched Ti–Cr alloys: (a) 30 at % Cr; (b) 40 at % Cr; (c) 50 at % Cr; (d) 60 at % Cr.

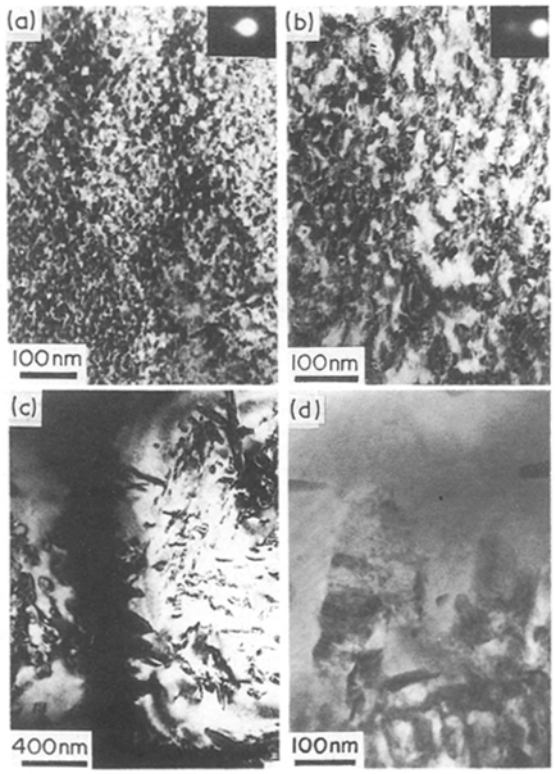


*Figure 3* TEM images and SAD patterns of liquid-quenched Ti–30 at % Cr alloy aged at 973 K for (a) 10 s, (b) 20 s, (c) 100 s, (d) 300 s.

Fig. 3 shows transmission electron micrographs and the 200 reflection spots of Ti–30Cr ribbons aged at 973 K. In the early stage of ageing, fine striations perpendicular to ⟨100⟩ are seen in the micrograph, and the 200 reflection spot is still accompanied by a

satellite, as shown in Fig. 3a. During short-term ageing, the space between the striations becomes wider, the 200 reflection spot splits into two and the satellite disappears, as shown in Fig. 3b. These facts indicate that the coherency between $\beta_1$ and $\beta_2$ is lost and the two phases coexist incoherently. During further ageing, the $\beta_1 + \beta_2$ two-phase structure coarsens, and new phases appear preferentially at grain boundaries and penetrate into the interior of the grains, as shown in Fig. 3c. These new phases are not yet identified fully, but one of them is $TiCr_2$ phase. Finally, the stable state of $\beta + TiCr_2$ is obtained as shown in Fig. 3d.

Fig. 4 shows the TEM images and the 200 reflection spot of Ti–40 Cr ribbons aged at 873 K. The changes during this ageing are similar to the case in Fig. 3, except for the final stable structure. First, fine striations perpendicular to $\langle 100 \rangle$ and a satellite around the 200 reflection spot appear (Fig. 4a). Next, the space of the striations becomes wide, i.e. the $\beta_1 + \beta_2$ structure coarsens, and the satellite becomes diffuse. Then the satellite disappears, the 200 reflection spot splits into two (Fig. 4b), and grain-boundary precipitates appear (Fig. 4c). Finally, stable phases of $\alpha$ and $TiCr_2$ completely cover all the ribbon.

Fig. 5 shows the TEM image and the SAD pattern of Ti–30Cr ribbon aged at 673 K for $1.8 \times 10^3$ s. In addition to the striations and the fundamental bcc reflection spots, some image contrast and diffuse scattering can be seen in the figure. These facts indicate that low-temperature ageing causes the formation of omega ($\omega$) phase in the $\beta_1 + \beta_2$ matrix of Ti–30Cr alloy. Fig. 6 shows the TEM image and the SAD pattern of Ti–50Cr ribbon aged at 973 K. Coherent $\beta_1 + \beta_2$ structure appears at first, as in the case of Ti–30Cr and Ti–40Cr ribbons. Then the coherent $\beta_1 + \beta_2$ structure transforms directly to the stable structure of $\alpha + TiCr_2$ or $\beta + TiCr_2$ without any loss in coherency.

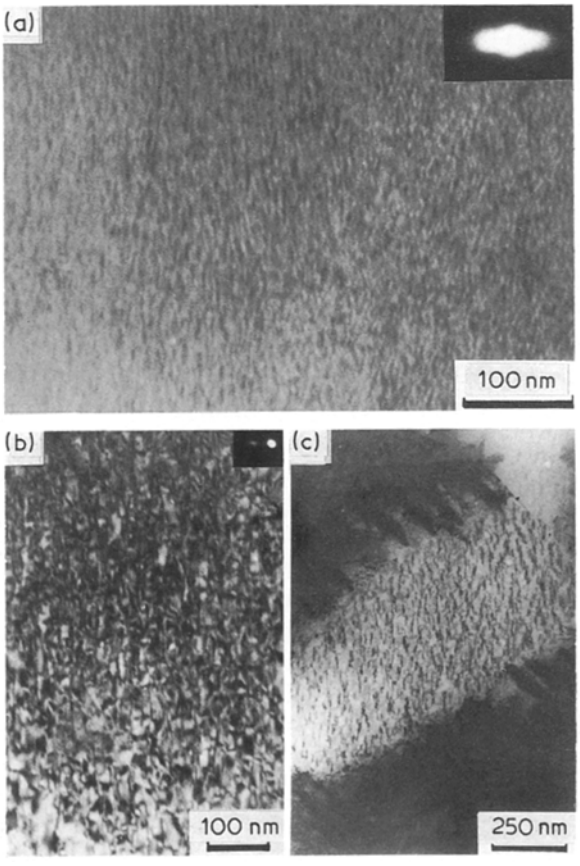


*Figure 4* TEM images and SAD patterns of liquid-quenched Ti–40 at % Cr alloy aged at 873 K for (a) 100 s, (b) 900 s, and (c) 1800 s.

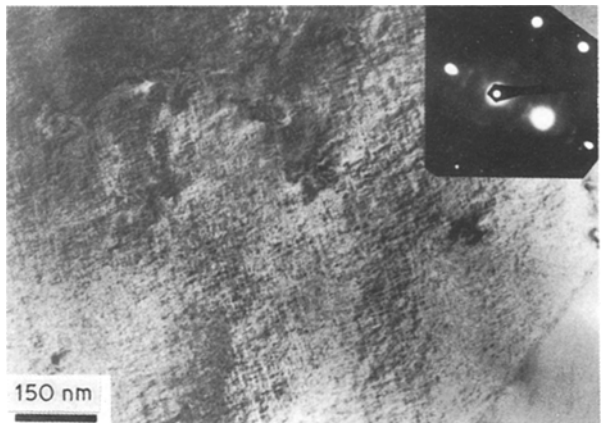


*Figure 5* TEM image and SAD pattern of liquid-quenched Ti–30 at % Cr alloy aged at 673 K for 1800 s.

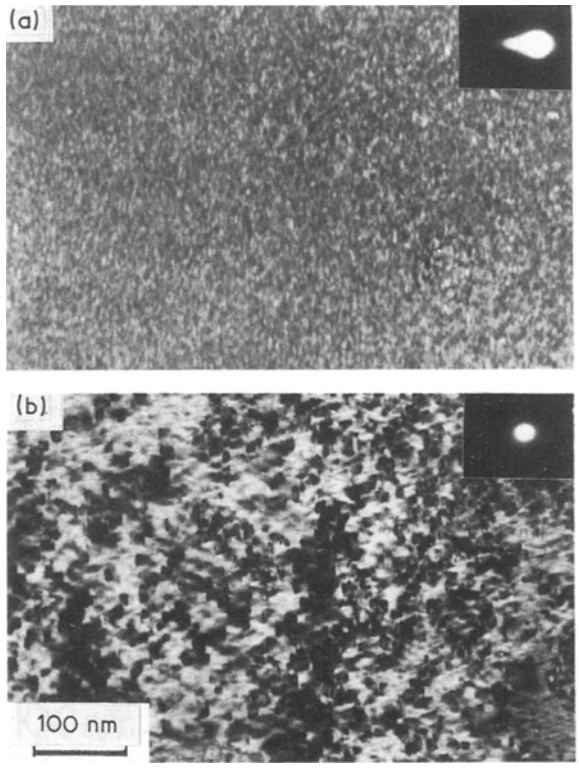


*Figure 6* TEM images and SAD patterns of liquid-quenched Ti–50 at % Cr alloy aged at 873 K for (a) 30 s and (b) 400 s.

## 4. Time–temperature–transformation (TTT) diagrams

During ageing of liquid-quenched β-type Ti–Cr alloys, six kinds of structure were observed:

(a) a two-phase structure of $\beta_1$ and $\beta_2$ which coexist coherently (coherent $\beta_1 + \beta_2$);

(b) a two-phase structure of $\beta_1$ and $\beta_2$ which coexist incoherently (incoherent $\beta_1 + \beta_2$);

(c) a stable two-phase structure of β and $TiCr_2$ ($\beta + TiCr_2$);

(d) a stable two-phase structure of α and $TiCr_2$ ($\alpha + TiCr_2$);

(e) a complex structure consisting of incoherent $\beta_1 + \beta_2$ and grain-boundary precipitates (incoherent $\beta_1 + \beta_2$ + GBP);

(f) a complex structure consisting of coherent $\beta_1 + \beta_2$ and ω-phase ($\beta_1 + \beta_2 + \omega$).

Figs 7–9 illustrate the TTT diagrams of β-type Ti–Cr alloys based on the TEM observations in the present studies. The broken lines in Figs 7 and 8 indicate the boundary between coherent and incoherent $\beta_1 + \beta_2$ two-phase fields. When the isothermal ageing reaches this curve, $\beta_1 + \beta_2$ structure loses the coherency.

In Ti–30Cr alloy (see Fig. 7), the two-phase field of $\beta_1 + \beta_2$ is broad, whether coherent or incoherent. A typical sequence of the structural change observed in this alloy is: coherent $\beta_1 + \beta_2 \rightarrow$ incoherent $\beta_1 + \beta_2 \rightarrow$ incoherent $\beta_1 + \beta_2 + GBP \rightarrow \alpha + TiCr_2$ or $\beta + TiCr_2$. At higher temperatures, stable phases are apt to appear during short-term ageing, and the coherent $\beta_1 + \beta_2$ state does not last so long. At lower temperatures, the $\beta_1 + \beta_2$ two-phase state is quite stable but the ω phase appears in the $\beta_1 + \beta_2$ matrix.

In Ti–40Cr alloy (see Fig. 8), the sequence of structural change is essentially the same as in the case of Ti–30Cr alloy. The main difference between Ti–40Cr and Ti–30Cr is that the grain-boundary precipitates in the former tend to appear more easily and more quickly than in the latter, and hence the $\beta_1 + \beta_2$ two-phase field in the TTT diagram is narrower for the former than the latter.

When the Cr-content is increased to 50 at %, the tendency for the precipitation at the grain boundary becomes higher, and hence two-phase field of $\beta_1 + \beta_2$ can be observed in the Ti–50Cr alloy (see Fig. 9). The solid curves in Figs 7–9 indicate the limit for the existence of $\beta_1 + \beta_2$ two-phase structure. When the ageing time exceeds this curve, $\beta_1 + \beta_2$ structure completely disappears. This limit does not change in practice even when the Cr-content varies between 30 and 50 at %.

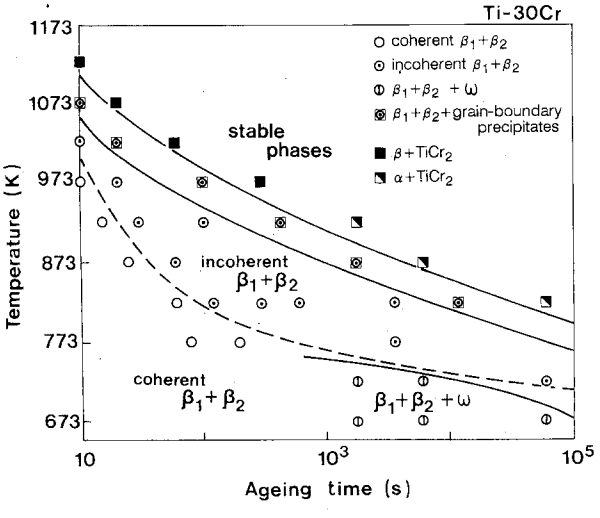


*Figure 7* TTT diagram of liquid-quenched Ti–30 at % Cr alloy.

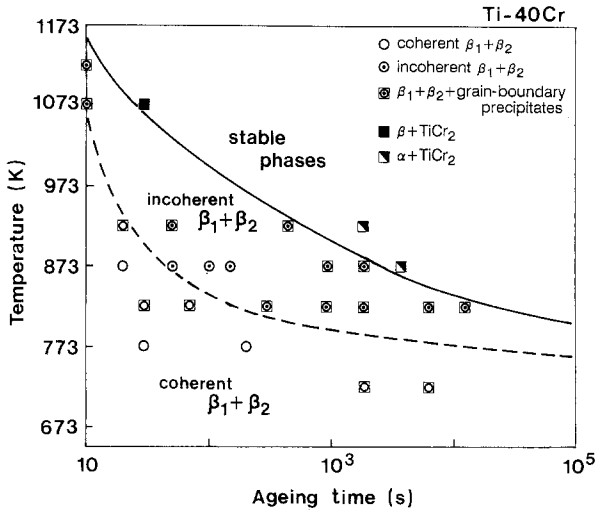


*Figure 8* TTT diagram of liquid-quenched Ti–40 at % Cr alloy.

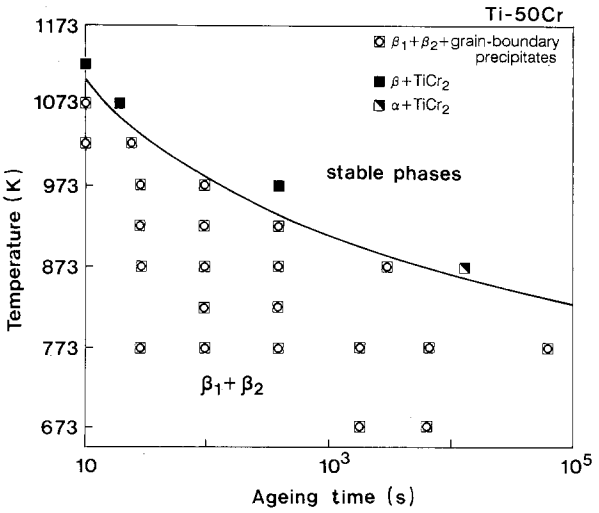


*Figure 9* TTT diagram of liquid-quenched Ti–50 at % Cr alloy.

## 5. Possibility of spinodal decomposition

Fig. 4a is representative of $\beta_1 + \beta_2$ two-phase structure in Ti–Cr alloys. Fine striations, which are perpendicular to ⟨100⟩ directions, and 200 or 220 reflection spots, which are accompanied by a set of symmetrical satellites along ⟨100⟩, indicate the existence of ⟨100⟩ modulated structure. Fig. 1 clearly indicates a remarkable age-hardening in a very short time. Such things are characteristic features of spinodal decomposition. Furthermore, Menon and Aaronson [9] suggested the occurrence of spinodal decomposition in the Ti–Cr system. Thus it was concluded that spinodal decomposition actually takes place in the β-phase of Ti–Cr alloy and the ⟨100⟩ modulated structure of $\beta_1 + \beta_2$ is a result of spinodal decomposition of the β-phase. It is apparent from Fig. 2 that the spinodal decomposition of β-phase proceeds too quickly to be suppressed even by liquid-quenching with a single-roll method.

Fig. 10 illustrates the two-phase field of $\beta_1 + \beta_2$ in the Ti–Cr system based on the present experimental studies. Each open circle indicates the maximum temperature at which $\beta_1 + \beta_2$ two-phase structure at each Cr-content was actually observed. Supercooled

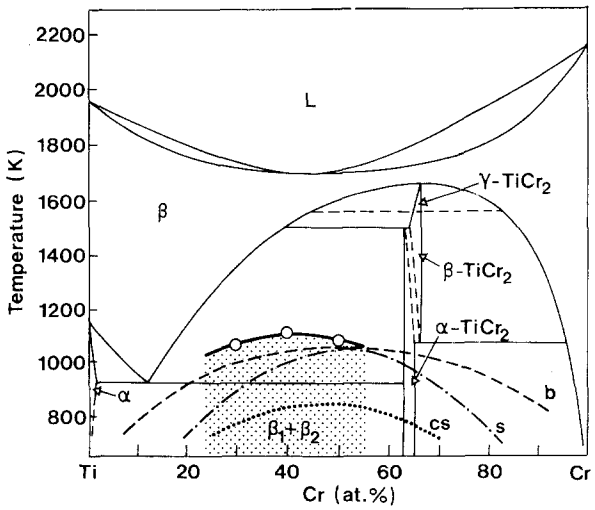


*Figure 10* Ti–Cr binary phase diagram showing the $\beta_1 + \beta_2$ two-phase field observed with TEM in the present studies (dotted area). (○) Highest temperature at which the $\beta_1 + \beta_2$ two-phase structure is observed for each composition. b, s and cs are the chemical binodal, the chemical spinodal and the coherent spinodal lines, respectively, which were calculated by Menon and Aaronson [9].

metastable β-phase decomposes to two phases of Ti-rich $\beta_1$ and Ti-lean $\beta_2$ in the dotted region of Fig. 10. The lines for chemical binodal (b), chemical spinodal (s) and coherent spinodal (cs), which Menon and Aaronson [9] calculated for β-type Ti–Cr alloys, are also drawn in the figure. The decomposition of β to $\beta_1 + \beta_2$ should take place at lower temperatures than the chemical binodal line. The present experimental results, however, indicate that phase decomposition actually takes place at higher temperatures than the calculated chemical binodal line. The reason why $\beta_1 + \beta_2$ two-phase field appears at such high temperatures is now under investigation.

## 6. Conclusions

1. A two-phase field of Ti-rich $\beta_1$ and Ti-lean $\beta_2$ spreads widely over the intermediate composition range of the binary Ti–Cr phase diagram. The $\beta_1 + \beta_2$ two-phase field expands towards higher temperatures than the chemical binodal line calculated by Menon and Aaronson [9].

2. A typical sequence of structural changes during ageing in the two-phase field is: β → coherent $\beta_1 + \beta_2$ → incoherent $\beta_1 + \beta_2$ → incoherent $\beta_1 + \beta_2$ + grain-boundary precipitates → stable state of $\beta + TiCr_2$ or $\alpha + TiCr_2$. Not all the states in the above sequence appear, depending on alloy composition, liquid-quenching rate and ageing temperature; in particular, the decomposition of β to $\beta_1 + \beta_2$ proceeds so quickly that $\beta_1$ and $\beta_2$ phases usually coexist coherently even in the as-liquid-quenched state.

3. The $\beta_1 + \beta_2$ two-phase state exhibits the so-called ⟨1 0 0⟩ modulated structure and such a structure is the result of spinodal decomposition of β-phase.

## Acknowledgement

The authors thank Dr T. Kozakai, Nagoya Institute of Technology, for considerable assistance.

## References

1. M. HANSEN and K. ANDERKO, "Constitution of Binary Alloys" (McGraw-Hill, New York, 1958).
2. F. L. HARMON and A. R. TROIANO, *Trans. Amer. Soc. Metals* **53** (1961) 43.
3. M. MIYAGI and S. SHIN, *J. Jpn Inst. Metals* **38** (1974) 455.
4. S. TERAUCHI, H. MATSUMOTO, T. SUGIMOTO and K. KAMEI, *ibid.* **41** (1977) 632.
5. T. B. MASSALSKI, J. L. MURRAY, L. H. BENNETT and H. BAKER, "Binary Alloy Phase Diagram", Vol. 2 (American Society for Metals, Metals Park, Ohio, 1986).
6. J. L. MURRAY, "Phase Diagrams of Binary Titanium Alloys" (American Society for Metals, Metals Park, Ohio, 1987).
7. G. H. NARAYANAN, T. S. LUHMAN, T. F. ARCHBOLD, R. TAGGART and D. H. POLONIS, *Metallography* **4** (1987) 343.
8. V. CHANDRASAKARAN, R. TAGGART and D. H. POLONIS, *ibid.* **6** (1973) 313.
9. E. S. MENON and H. I. AARONSON, *Acta Metall.* **34** (1986) 1963.

*Received 30 October 1989*
*and accepted 24 April 1990*